Journal of Hazardous Materials 167 (2009) 193–198

Contents lists available at ScienceDirect

Journal of Hazardous Materials

journal homepage: www.elsevier.com/locate/jhazmat

Biodegradation kinetics of picric acid by *Rhodococcus* sp.NJUST16 in batch reactors

Jinyou Shen, Rui He, Lianjun Wang*, Jianfa Zhang, Yi Zuo, Yanchun Li, Xiuyun Sun, Jiansheng Li, Weiqing Han

School of Chemical Engineering, Nanjing University of Science and Technology, 200 Xiaolingwei Street, Nanjing 210094, Jiangsu Province, China

ARTICLE INFO

Article history:
Received 9 September 2008
Received in revised form
25 November 2008
Accepted 22 December 2008
Available online 30 December 2008

Keywords:
Rhodococcus
Picric acid
Biodegradation
Kinetic parameters
Substrate inhibition

ABSTRACT

Biological degradation of 2,4,6-trinitrophenol (TNP) by *Rhodococcus* sp.NJUST16 in mineral salt medium was investigated in shake-flask experiments at pH of 7.0 and 30°C, over a wide range of initial TNP concentration (20–800 mg l^{-1}). The TNP was observed to be the inhibitory compound. For the studied concentration range, Haldane's model could be fitted to the growth kinetics data well with the kinetic constants μ_{max} = 0.2362 h^{-1}, K_s = 9.9131 mg l^{-1} and K_i = 362.7411 mg l^{-1}. Further, the variation of observed yield coefficient Y with initial TNP concentration and the decay coefficient were investigated. It is our view that the above information would be useful for modeling and designing the units treating TNP-containing wastewaters.

1. Introduction

Aqueous nitrophenolic effluents are relatively common industrial wastes, being produced in the manufacture and processing of a variety of industrial products, such as pesticides, herbicides, explosives, dyes and plasticizers, etc. [1,2]. Nitrophenols are difficult to be decomposed biologically, and are toxic to plants, microorganisms, animals and humans, causing serious environmental problems [3,4]. US Environmental Protection Agency (EPA) rated nitrophenol as priority pollutant and recommended restricting its concentration in the natural water bodies to below 10 ng ml^{-1} [1,5].

As a result of growing awareness over pollution caused by nitrophenols release, efforts are being made to minimize their adverse effect. Many treatment technologies such as advanced oxidation processes (AOPs) [6,7], extraction [8], adsorption [9], and biological treatment [10–12] have been developed to remove nitrophenols from contaminated environment. Of these options, physicochemical methods have proven to be costly and have the inherent drawbacks of causing a secondary pollution. However, biological method treatment, which is environmental friendly and cost effective, has turned out to be a favorable alternative [13,14].

However, the presence of substituted groups, i.e., nitro-, on phenols increases the toxic effects on ecosystem and human health due to their persistence in the environment [4]. Due to the pronounced electron-withdrawing character of the nitro groups, nitroaromatics, particularly polynitroaromatics like 2,4,6-trinitrophenol (TNP), harbor a highly electron deficient π-electron system [15]. The electrophilic attack which is usually the first step in aromatic biodegradation becomes more difficult. As a result, polynitroaromatic compounds are subject to initial reductive transformation. They are more resistant to mineralize [10,15–17]. Hence, the number of TNP-degrading bacteria is small. Knowledge about TNP degradation is yet limited.

What is more, knowledge of the kinetics of biodegradation is important for the evaluation of the persistence of organic pollutants and the design of biodegradation facilities [18,19]. Mathematical modeling can be helpful for understanding the behaviour of biological processes and predicting the component concentrations in the system. However, to best of our knowledge, the growth kinetics of these TNP-degrading isolates has been seldom investigated in the previous studies.

We have isolated a strain of *Rhodococcus* sp. from a site contaminated by TNP at the Nanjing Taowu Chemical Factory in China and utilized it for biological degradation of TNP [20]. In this article, a clarification and quantitative discussion of the relationship between specific growth rate and substrate concentration, a consideration of variable cell mass yield as well as the decay coefficient will be presented. The Haldane's model will be validated experimentally over a wide range of initial TNP concentrations.

* Corresponding author. Tel.: +86 25 84315518; fax: +86 25 84315518.
E-mail address: wanglj@mail.njust.edu.cn (L. Wang).

0304-3894/$ – see front matter © 2008 Elsevier B.V. All rights reserved.
doi:10.1016/j.jhazmat.2008.12.100

Nomenclature

k_d	decay coefficient (h^{-1})
K_i	Haldane's growth kinetics inhibition coefficient ($mg\,l^{-1}$)
K_s	half saturation coefficient ($mg\,l^{-1}$)
R^2	correlation coefficient (−)
S	concentration of substrate ($mg\,l^{-1}$)
t	time (h)
X	concentration of biomass ($mg\,l^{-1}$)
Y	observed yield coefficient (mg biomass/mg substrate)

Greek letters

μ_g	specific growth rate (h^{-1})
μ_{max}	maximum specific growth rate (h^{-1})
μ_{net}	$\mu_g - k_d$, net specific growth rate (h^{-1})

Subscript

0	initial value

2. Kinetics models development

In our work, as the flasks were covered with six layer gauzes, it was presumed that the aeration provided by shaking the flasks was able to keep the oxygen concentration sufficient and not limited, the influence of oxygen was not considered. Thus, the *Rhodococcus* sp. growth rate and TNP degradation rate were only limited by substrate concentration at fixed initial pH, temperature and shaking rate.

Cell growth kinetics in a batch reactor may be modeled by the following equation:

$$\frac{dX}{dt} = \mu_g X - k_d X = \mu_{net} X \quad (1)$$

For substrate,

$$\frac{dS}{dt} = -\frac{1}{Y}\left(\frac{dX}{dt}\right) \quad (2)$$

μ_g is a function of S. In the literature, two approaches are mostly encountered for representing the kinetics of bacterial growth on substrates. According to one, substrates are considered noninhibitory compounds and so are represented by Monod's noninhibitory kinetics equation as given below:

$$\mu_g = \frac{\mu_{max} S}{K_s + S} \quad (3)$$

The other view considers the substrates to be growth inhibitory compounds. Of the kinetics models describing the growth kinetics of inhibitory compound, Haldane's model is widely studied due to its mathematical simplicity and wide acceptance for representing the growth kinetics of inhibitory substrates. The Haldane's inhibitory growth kinetics equation is as follows:

$$\mu_g = \frac{\mu_{max} S}{K_s + S + (S^2/K_i)} \quad (4)$$

At higher substrate concentrations, $S \gg K_s$, the above equation reduces to the following:

$$\mu_g = \frac{\mu_{max} S}{S + (S^2/K_i)} \quad (5)$$

or

$$\frac{1}{\mu_g} = \frac{1}{\mu_{max}} + \frac{S}{(K_i \mu_{max})} \quad (6)$$

This is the linearized Haldane's equation.

The time profiles of substrate degradation prediction can be done by combining Eqs. (1), (2) and (4):

$$\frac{1}{X}\frac{dS}{dt} = -\frac{1}{Y}\left(\frac{\mu_{max} S}{K_s + S + (S^2/K_i)}\right) \quad (7)$$

Also, it can be assumed that endogenous coefficient k_d in Eq. (1) may be neglected during exponential phase. Eq. (1) therefore reduces to the following equation:

$$\frac{dX}{dt} = \mu_g X \quad (8)$$

During initial phase, S may be taken equal to S_0. Therefore,

$$\ln\left(\frac{X}{X_0}\right) = \mu_g t \quad (9)$$

3. Materials and methods

3.1. Microorganism and culture media

Pure culture of *Rhodococcus* sp.NJUST16 was used throughout our work. *Rhodococcus* sp.NJUST16 was isolated in this lab previously and identified based on Gram staining, biochemical tests, and 16S rRNA sequence determination [20]. The 16S rRNA sequence was deposited in the GenBank database under accession no. EF635425. Store culture of this strain was maintained by periodic sub transfer on mineral salt agar plates supplemented with 500 $mg\,l^{-1}$ TNP and stored at 4 °C.

The liquid mineral salt (MS) medium used in this study contained $Na_2HPO_4{\cdot}12H_2O$ (3.057 $g\,l^{-1}$), KH_2PO_4 (0.743 $g\,l^{-1}$), $MgSO_4{\cdot}7H_2O$ (0.2 $g\,l^{-1}$), $CaCl_2$ (0.05 $g\,l^{-1}$), SL-4 (10 $ml\,l^{-1}$) and a certain amount of TNP stock solution. The composition of SL-4 was described previously [20]. The TNP stock solution contained 4000 $mg\,l^{-1}$ TNP, and was adjusted to pH 7.0 with 1 $mol\,l^{-1}$ of NaOH. The initial pH of the medium was 7.0. 50 ml of the media was transferred to 150 ml of an Erlenmeyer flask and autoclaved at 121 °C for 20–30 min.

3.2. Experimental procedures

The inocula for the experiments of TNP degradation study were prepared as follows [20]: the mineral salts medium supplemented with 500 $mg\,l^{-1}$ TNP, was inoculated with pure culture of NJUST16 and incubated at 30 °C on a shaker at 180 rpm. 2 ml of this cell culture was added to fresh medium as inoculum. 32 h later, a third fresh medium was also inoculated with 2 ml of the last culture, ensuring that bacteria were already adapted to TNP. The induced cells at late exponential growth phase (cell concentration of about 2×10^7 cells/ml, OD_{600} around 0.3 absorbance units) were then transferred to each experimental flask containing the prepared medium as the inocula.

To investigate the influence of inoculum volume on phenol degradation, 50 ml mineral media with 500 $mg\,l^{-1}$ TNP were inoculated with the inocula of 1 ml, 2 ml, 3 ml, 4 ml, respectively. For determination of the kinetic parameters, the degradation experiments were conducted with a series of 150 ml Erlenmeyer flask with 50 ml MS media supplemented with various TNP concentrations. All the reactors were inoculated with 2 ml inocula described above. Initial TNP concentrations varied from 20 to 100 $mg\,l^{-1}$ at an interval of 20 $mg\,l^{-1}$, and 100–800 $mg\,l^{-1}$ at an interval of 100 $mg\,l^{-1}$. All of above experiments were carried out at initial pH of 7.0 and 30 °C (as previous study [20] indicated, NJUST16 grew optimally at

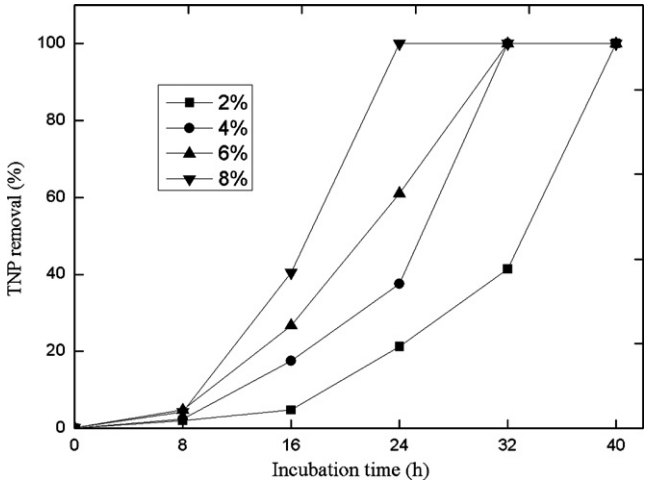

Fig. 1. Effect of the inoculum size on TNP degradation.

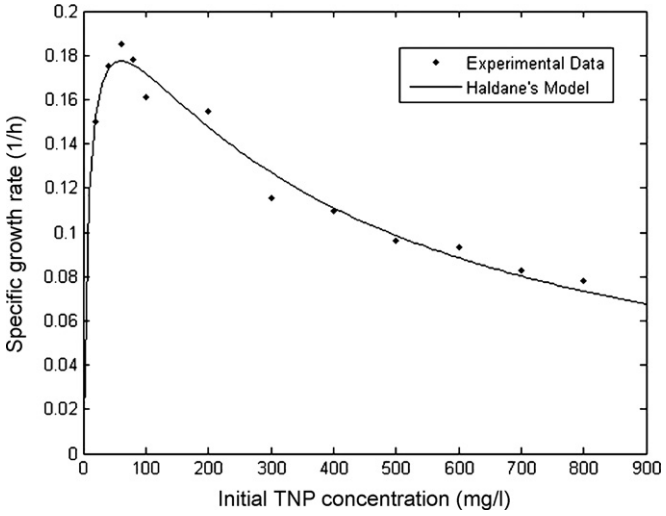

Fig. 2. Experimental and predicted specific growth rates of the culture due to Haldane's model.

this conditions) on a shaker at 180 rpm. The variation of TNP concentration and the OD of growth were monitored at suitable time intervals throughout the study.

3.3. Analytical methods

To determine the amount of remaining TNP, samples were passed through a 0.22 μm filter and submitted to analysis. TNP in the supernatant were identified and quantified by HPLC (Waters 2996, Waters Incorporation, USA) conducted at room temperature using Waters RP18 column (5 μm, 3.9 mm × 150 mm) and a diode array detector at a flow rate of 1.00 ml min^{-1}. The mobile phase consisted of 30% acetonitrile, 70% water and 0.26% H_3PO_4 (v/v/v). The analysis was performed at 254 nm, column temperature at 35 °C. The optical density (OD) of cell growth was determined at 600 nm using a UV-VIS Spectrophotometer (TU-1901, Purkinje General Instrument Co. Ltd., China) throughout the studies. As the culture supernatant turned red during fermentation, a cell free sample of the corresponding supernatant was used as the blank. The OD value was then converted to dry cell mass using a dry weight calibration curve obtained by plotting dry weight of biomass per liter against optical density of the suspension. The pH was measured in a pH meter (PHS-3B, Shanghai Precision & Scientific Instrument Co. Ltd., China).

4. Results and discussion

4.1. Effect of inoculum size on TNP degradation

Fig. 1 indicated the effect of inoculum volume on TNP degradation. The MS media inoculated with 8% starting inoculum underwent a shortest lag phase, and manifested the highest TNP-degrading velocity. The results showed that the increased inoculum concentration reduced the lag phase and helped the system to reach the exponential growth phase quickly.

4.2. Effect of initial concentration on strain growth

In order to evaluate the effect of initial concentration on strain growth, the specific growth rate (μ) for each value of the initial TNP concentration (S_0), was determined in the exponential growth phase. In these experiments initial TNP concentrations varied in the range 20–800 mg l^{-1}. After a lag phase, linear plots were obtained at all initial concentrations, which indicated that the TNP was the limiting substrate in this region and the culture was growing exponentially. The OD of cell growth was monitored continuously. The natural logarithm of these measurements was plotted against the incubation time, and the growth rates were calculated by using Eq. (9). In the present research work, such plots had been used for the determination of specific growth rates at different initial TNP concentrations.

The experimental specific growth rate data were plotted against initial concentration of TNP. Fig. 2 showed a typical trend that the value of specific growth rate increased with the increase in initial TNP concentration up to a certain concentration level, then it started decreasing with the increase in the concentration. From this figure, the value of maximum specific growth rate was found to be equal to 0.1850 h^{-1}, it was achieved at initial TNP concentration of about 60 mg l^{-1}. The decline trend of the plot beyond 60 mg l^{-1} indicated that TNP was inhibitory type substrate and the inhibition effect of TNP become predominant above 60 mg l^{-1}.

4.3. Determination on kinetic parameters

In order to estimate the kinetic parameters of TNP, Haldane's growth kinetics model was used. In general, Haldane's growth kinetics model was used to represent growth kinetics data of an inhibitory compound such as phenol. The model had been used on the premise that this had less number of parameters and lent itself to be used easily in model equations [21]. However, the estimation of these three parameters values required the use of a nonlinear least squares technique.

In this study, the parameters were obtained by a nonlinear least squares technique using MATLAB 7.0, based on Windows XP. Experimental and predicted specific growth rates of the culture due to Haldane's model were shown in Fig. 2. Values of kinetic constants for TNP degradation obtained in this work were listed in Table 1. The μ_{max} and K_s values reported in other literatures for TNP degradation were also included. In general, μ_{max} value reported in this work was much larger than those estimated in the literature. The large value of μ_{max} indicated that substrate was degraded by microorganism more rapidly. The magnitude of K_s value indicated the affinity of biomass to substrate. The low value of K_s indicated the high affinity of biomass to substrate and so growth rate was high. In the study in Table 1, K_s values fell in the range of 25–50 mg l^{-1} with an exception of 0.68 mg l^{-1}. While K_s value, obtained for this study was 9.9131 mg l^{-1}. The low value of K_s implied that the affinity of NJUST16 to degrade TNP at prevailing operating conditions was relatively high. The evident variability seen in the literature for

Table 1
Reported value of μ_{max}, K_s and K_i for TNP.

μ_{max} (h^{-1})	K_s ($mg\,l^{-1}$)	K_i ($mg\,l^{-1}$)	T (°C)	System	Cultures	Reference
0.005	0.68		25	Aerobic sequencing batch reactor	*Rhodococcus opacus* strain JW01	[22]
0.05	50		25	Membrane enhanced biofilm reactor	*Nocardioides simplex* strain Nb	[23]
0.05	25		25	Membrane enhanced biofilm reactor	*Nocardioides simplex* strain Nb	[23]
0.06	50		25	Membrane enhanced biofilm reactor	*Nocardioides simplex* strain Nb	[23]
0.2362	9.9131	362.7411	30	Batch	*Rhodococcus* sp.NJUST16	This work

these biokinetic constant values may be due to various factors such as inoculum history, changes in predominating microbial species and different environmental factors [24]. However, the magnitudes of kinetic parameter K_i, which indicated both the inhibition tendency of the substrate and the degree of toxicity of the substrate in the medium towards the microorganisms, were still lacking in the present literature. The K_i value of 362.7411 $mg\,l^{-1}$ was comparable to the phenol degradation systems in the literature [25].

It was known that TNP was truly xenobiotic. Nitrophenols were difficult to be decomposed biologically, and were more toxic to microorganisms than phenol. However, The μ_{max}, K_s and K_i value (0.2362 h^{-1}, 9.9131 $mg\,l^{-1}$ and 362.7411 $mg\,l^{-1}$) obtained in this work all lay in the range of literature results (0.119–0.542 h^{-1}, 1.06–44.92 $mg\,l^{-1}$, 54.1–934.5 $mg\,l^{-1}$) [25]. It implied that at given operating conditions, the TNP biodegradation potential of *Rhodococcus* sp.NJUST16 was comparable with that of other popular microorganisms to treat phenolic waste in the literature.

4.4. Yield coefficient

The cell mass yield coefficient (dry weight of biomass/weight of substrate) was estimated by linearizing cell mass density increase with phenol consumption, as is given below:

$$Y = \frac{X_m - X_0}{S_s - S_0} \tag{10}$$

Fig. 3 plotted the cell mass yield coefficient as a function of initial TNP concentration. As initial TNP concentration varied from 20 to 900 $mg\,l^{-1}$, the yield coefficient varied between 0.1424 $g\,g^{-1}$ and 0.3215 $g\,g^{-1}$, and seemed to be too low (Fig. 3). It is probably due to the following reasons [16]: (1) a considerable portion of the molecular weight of TNP was provided by the three nitro groups; and (2) at least two NADPH molecules had to be used to remove the nitro groups from the aromatic system. However, these values are comparable with these data obtained by Behrend and Heesche-Wanger [16].

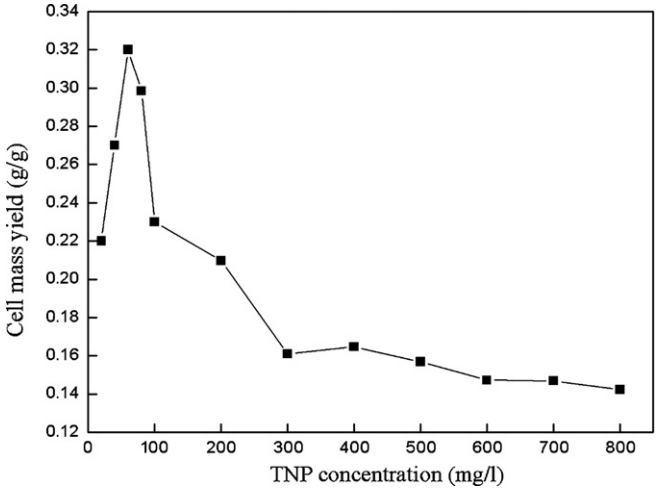

Fig. 3. Effect of initial TNP concentrations on cell mass yield.

Besides, the profile of cell mass yield as a function of initial TNP concentration was similar to that of specific growth rate (Figs. 2 and 3). The yield maximized at TNP concentration of 60 $mg\,l^{-1}$ where μ was also maximum. Beyond 60 $mg\,l^{-1}$, considerable decrease in the values of mass yield coefficient was observed with increase in TNP concentration up to 800 $mg\,l^{-1}$. Similar results of decreasing Y with increasing substrate concentration in inhibitory region were also reported in the literature [14,26,27]. This phenomenon could be reasoned based on the fact that the percentage of the total substrate carbon converted to energy for cell growth and maintenance increased as the specific growth rate decreased, when the inhibition effect of TNP become predominant above initial TNP concentration of 60 $mg\,l^{-1}$. More energy was required to overcome the effect of substrate inhibition during the degradation of TNP. While the percentage of the total substrate carbon assimilated into biomass decreased as the specific growth rate decreased. In addition, the production and accumulation of intermediates may also be responsible for the decreased cell mass yield. Thus substrate inhibition was known not only to reduce the specific growth rate, but also to reduce cell growth yield.

4.5. Endogenous or decay coefficient

The endogenous decay described the conversion of cell mass into maintenance energy. The decay coefficient affected the growth kinetics because it appeared in the mass balance equation of the cell growth (Eq. (1)). A typical growth curve showed a decline in cell population after the complete consumption of substrate. During this declining phase some parts of the cell population become food for the rest of the cell population. This part of the growth curve in a batch reactor had been modeled by following equation.

$$\frac{dX}{dt} = -k_d X \tag{11}$$

In order to determine the value of k_d, the growth of culture was continued and the cell mass concentration was observed for another 24 h even after the complete consumption of TNP. The experiment was conducted for initial TNP concentration of 500 $mg\,l^{-1}$. The selection of the particular growth run was arbitrary, assuming that the k_d value is not dependent on initial TNP concentration. Fig. 4 showed the batch growth curves extended up to endogenous region at initial TNP concentration of 500 $mg\,l^{-1}$. Fig. 5 showed the data of the endogenous region plotted as $\log_e$ (optical density) versus time. The negative slope gave decay rate coefficient. The value of the decay rate coefficient obtained in this study was 0.01713 h^{-1} for TNP degradation. While the decay rate coefficient values for *Pseudomonas putida* MTCC 1194 in phenol and catechol biodegradation system described by Kumar et al. [21] were 0.0056 and 0.0067 h^{-1}, respectively. The decay rate coefficient for NJUST16 in this study was larger than that for *P. putida* MTCC 1194. The growth rate would be reduced by as much the value of decay coefficient so that the wash out condition would occur at lower dilution rates.

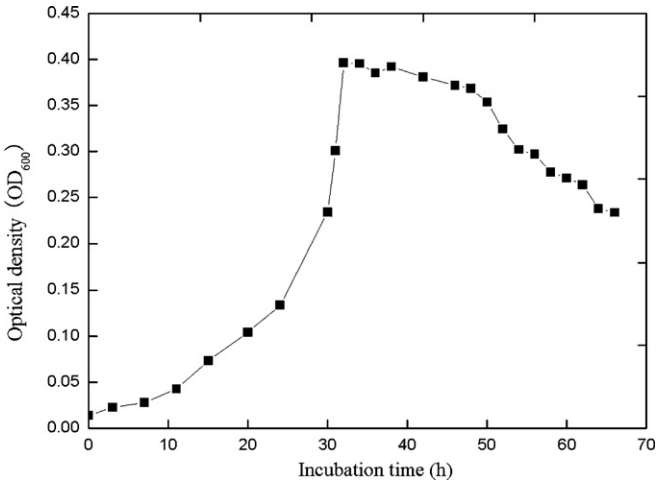

Fig. 4. Batch growth curve extended up to decay phase for TNP degradation by *Rhodococcus* sp.NJUST16 at initial TNP concentration of 500 mg l^{-1}.

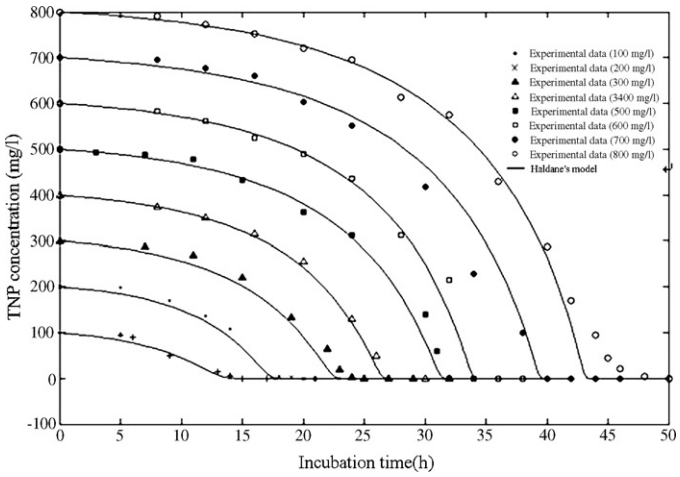

Fig. 6. Comparison of computer simulations by Haldane's model and experimental data for different initial TNP concentrations.

4.6. Simulations with the Haldane model

TNP degradation was modeled by Eqs. (4), (7) and (9). Simulations were performed for studied initial TNP concentration in the range of 100–900 mg l^{-1}. Kinetic values of the Haldane equation used in simulations were $\mu_m = 0.2362\ h^{-1}$, $K_s = 9.9131$ mg l^{-1} and $K_i = 362.7411$ mg l^{-1}. Y and μ values at various initial concentration of TNP had been described previously. X_0 was calculated using a dry weight calibration curve, and equaled to 2.9 mg l^{-1}.The degradation profiles of TNP could be simulated at different initial TNP concentrations. The results of the comparison between the simulations and the experimental data were presented in Fig. 6. It could be seen that the model predictions fitted the experimental data well.

It was noteworthy that there was a region of relatively less rate of substrate removal at the end of the TNP degradation curve, at an initial TNP concentration of 800 mg l^{-1} (Fig. 6). While at TNP concentration of 900 mg l^{-1}, degradation was incomplete with about 89% of TNP degraded after 48 h, but no further degradation was observed for a longer time [20]. Although phosphate buffer was present in the media, pH decreased from 7.0 to 6.23 at the end of study with the initial TNP concentration of 900 mg l^{-1}. pH decreased from 7.0 to 6.36 at the end of study with the initial TNP concentration of 800 mg l^{-1}. We inferred that the fall in pH of the solution may be the main reason [20]. In addition, for the TNP degradation pathway by NJUST16, the mechanism involved addition of hydride ion to the aromatic system followed by ring fission and elimination of nitrite, forming carboxylic acids which are readily susceptible to biodegradation [20]. The degradation of TNP by NJUST16 was accompanied by release of stoichiometric amount of nitrite and acidification, forming nitrous acid (HNO_2), which was toxic [20,28,29]. The degradation of TNP by NJUST16 was inhibited by HNO_2 generated at the end of the degradation, at high initial TNP concentration.

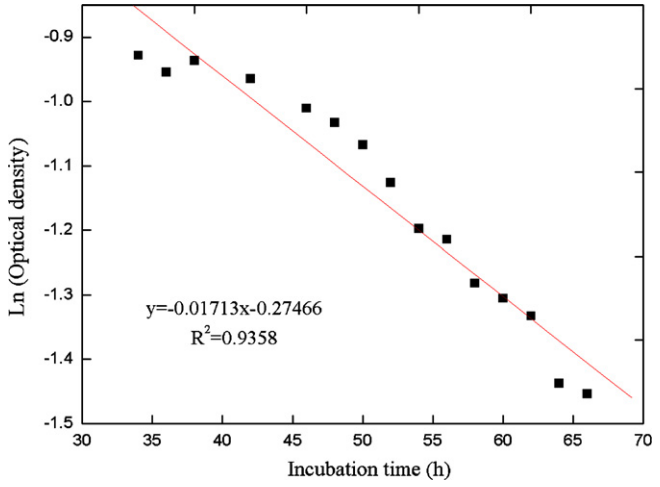

Fig. 5. Evaluation of decay coefficient k_d for *Rhodococcus* sp.NJUST16 growth on TNP using decay phase batch growth experimental data.

5. Conclusions

Picric acid, as the sole carbon, nitrogen and energy source, could be degraded by *Rhodococcus* sp.NJUST16 over a wide concentration range of 20–800 mg l^{-1}.

For batch experiments carried out, at 30 °C and initial pH of 7.0, Haldane's model was discussed in order to simulate the TNP removal profile with time. The kinetic constants of the Haldane's equation were $\mu_{max} = 0.2362\ h^{-1}$, $K_s = 9.9131$ mg l^{-1} and $K_i = 362.7411$ mg l^{-1}. The cell mass yield coefficient decreased with increasing substrate concentration in inhibitory region. The decay coefficient was found to be 0.01713 h^{-1} for NJUST16. The Haldane's model fitted TNP degradation profiles well with only one set of model parameters.

The maximum specific growth rate of *Rhodococcus* sp.NJUST16, μ_{max}, was higher than that observed by other researchers. This led to higher efficiencies when using *Rhodococcus* sp.NJUST16 for TNP degradation. The low value of K_s implied that the affinity of NJUST16 to degrade TNP at prevailing operating conditions was relatively high.

Acknowledgements

This research is financed by Foundational Research Program of the Civilian Blasting and Research Innovation Grant for Graduate of Common High School of Jiangsu Province (AD20246). We thank Yue Zhao and Ying Zhang for bacterial identification, Rui Li for technical assistance in HPLC.

References

[1] M. Kulkarni, A. Chaudhari, Biodegradation of *p*-nitrophenol by *P. putida*, Bioresour. Technol. 97 (2006) 982–988.
[2] J.C. Spain, Biodegradation of nitroaromatic compounds, Annu. Rev. Microbiol. 49 (1995) 523–555.

[3] T. Hirooka, H. Nagase, K. Hirata, K. Miyamoto, Degradation of 2,4-dinitrophenol by a mixed culture of photoautotrophic microorganisms, Biochem. Eng. J. 29 (2006) 157–162.
[4] N.S. Wan, J.D. Gu, Y. Yan, Degradation of *p*-nitrophenol by *Achromobacter xylosoxidans* Ns isolated from wetland sediment, Int. Biodeterior. Biodegrad. 59 (2007) 90–96.
[5] US Environment Protection Agency, Water quality criteria, Washington, DC 1976, US Environmental Protection Agency.
[6] O. Gimeno, M. Carbajo, F.J. Beltran, F.J. Rivas, Phenol and substituted phenols AOPs remediation, J. Hazard. Mater. B119 (2005) 99–108.
[7] F.R. Zaggout, N.A. Ghalwa, Removal of *o*-nitrophenol from water by electrochemical degradation using a lead oxide/titanium modified electrode, J. Environ. Manage. 86 (2008) 291–296.
[8] J. Luan, A. Plaisier, Study on treatment of wastewater containing nitrophenol compounds by liquid membrane process, J. Memb. Sci. 229 (2004) 235–239.
[9] D. Tang, Z. Zheng, K. Lin, J. Luan, J. Zhang, Adsorption of *p*-nitrophenol from aqueous solutions onto activated carbon fiber, J. Hazard. Mater. 143 (2007) 49–56.
[10] J.L. Ramos, M.M. González-Pérez, A. Caballero, P. van Dillewijn, Bioremediation of polynitrated aromatic compounds: plants and microbes put up a fight, Curr. Opin. Microbiol. 16 (2005) 275–281.
[11] S.K. Samanta, B. Bhushan, A. Chauhan, R.K. Jain, Chemotaxis of a *Ralstonia* sp. SJ98 toward different nitroaromatic compounds and their degradation, Biochem. Biophys. Res. Commun. 269 (2000) 117–123.
[12] M.C. Tomei, M.C. Annesini, R. Luberti, G. Cento, A. Senia, Kinetics of 4-nitrophenol biodegradation in a sequencing batch reactor, Water Res. 37 (2003) 3803–3814.
[13] R.S. Juang, S.Y. Tsai, Growth kinetics of *Pseudomonas putida* in the biodegradation of single and mixed phenol and sodium salicylate, Biochem. Eng. J. 31 (2006) 133–140.
[14] R.K. Singh, S. Kumar, S. Kumar, A. Kumar, Biodegradation kinetic studies for the removal of p-cresol from wastewater using *Gliomastix indicus* MTCC 3869, Biochem. Eng. J. 40 (2008) 293–303.
[15] P.G. Rieger, H.M. Meier, M. Gerle, U. Vogt, T. Groth, H.J. Knackmuss, Xenobiotics in the environment: present and future strategies to obviate the problem of biological persistence, J. Biotechnol. 94 (2002) 101–123.
[16] C. Behrend, K. Heesche-Wanger, Formation of Hydride-Meisenheimer complexes of picric acid (2,4,6-trinitrophenol) and 2,4-dinitrophenol during mineralization of picric acid by *Nocardioides* sp. strain CB 22-2, Appl. Environ. Microbiol. 65 (1999) 1372–1377.
[17] G. Heiss, K.W. Hofmann, N. Trachtmann, D.M. Walters, P. Rouvière, H.J. Knackmuss, *npd* gene functions of *Rhodococcus (opacus) erythropolis* HL PM-1 in the initial steps of 2,4,6-trinitrophenol degradation, Microbiology 148 (2002) 799–806.
[18] J. Bai, J.P. Wen, H.M. Li, Y. Jiang, Kinetic modeling of growth and biodegradation of phenol and *m*-cresol using *Alcaligenes faecalis*, Process Biochem. 42 (2007) 510–517.
[19] K.C. Loh, Y.G. Yu, Kinetics of carbazole degradation by *Pseudomonas putida* in presence of sodium salicylate, Water Res. 34 (2000) 4131–4138.
[20] J. Shen, J. Zhang, Y. Zuo, L. Wang, X. Sun, J. Li, W. Han, R. He, Biodegradation of 2,4,6-trinitrophenol by *Rhodococcus* sp. isolated from a picric acid-contaminated soil, J. Hazard. Mater. 163 (2009) 1199–1206.
[21] A. Kumar, S. Kumar, S. Kumar, Biodegradation kinetics of phenol and catechol using *Pseudomonas putida* MTCC 1194, Biochem. Eng. J. 22 (2005) 151–159.
[22] J.L. Weidhaas, E.D. Schroeder, D.P. Chang, An aerobic sequencing batch reactor for 2,4,6-trinitrophenol (picric acid) biodegradation, Biotechnol. Bioeng. 97 (2007) 1408–1414.
[23] S.J. Grimberg, M.J. Rury, K.M. Jimenez, A.K. Zander, Trinitrophenol treatment in a hollow fiber membrane biofilm reactor, Water Sci. Technol. 41 (2000) 235–238.
[24] A. Nuhoglu, B. Yalcin, Modelling of phenol removal in a batch reactor, Process Biochem. 40 (2005) 1233–1239.
[25] P. Saravanan, K. Pakshirajan, P. Saha, Growth kinetics of an indigenous mixed microbial consortium during phenol degradation in a batch reactor, Bioresour. Technol. 99 (2008) 205–209.
[26] F. Chen, M.R. Johns, Relationship between substrate inhibition and maintenance energy of *Chlamydomonas reinhardtii* in heterotrophic culture, J. Appl. Phycol. 8 (1996) 15–19.
[27] S.J. Wang, K.C. Loh, Modeling the role of metabolic intermediates in kinetics of phenol biodegradation, Enzyme Microb. Technol. 25 (1999) 177–184.
[28] C. Glass, J. Silverstein, Denitrification kinetics of high nitrate concentration water: pH effect on inhibition and nitrite accumulation, Water Res. 32 (1998) 831–839.
[29] C. Glass, J. Silverstein, Denitrification of high-nitrate, high-salinity wastewater, Water Res. 33 (1999) 223–229.